Am. J. Hum. Genet. 69:1370–1377, 2001

Report

Large-Scale Deletions and *SMADIP1* Truncating Mutations in Syndromic Hirschsprung Disease with Involvement of Midline Structures

Jeanne Amiel,[1] Yolanda Espinosa-Parrilla,[1] Julie Steffann,[1] Philippe Gosset,[1] Anna Pelet,[1] Marguerite Prieur,[1] Odile Boute,[2] Agnès Choiset,[3] Didier Lacombe,[4] Nicole Philip,[5] Martine Le Merrer,[1] Hajime Tanaka,[6] Marianne Till,[7] Renaud Touraine,[8] Annick Toutain,[9] Michel Vekemans,[1] Arnold Munnich,[1] and Stanislas Lyonnet[1]

[1]Département de Génétique, et Unité INSERM U-393, Hôpital Necker-Enfants Malades, and [2]Service de Cytogénétique, Hôpital Saint Vincent de Paul, Paris; [3]Service de Pédiatrie, Hôpital Huriez, Lille; [4]Service de Génétique, Hôpital Pellegrin, Bordeaux; [5]Département de Génétique, Hôpital d'Enfants de la Timone, Marseille; [6]Department of Pediatrics, Asahikawa Habilitation Center for Disabled Children, Asahikawa, Japan; [7]Service de Pédiatrie, Hôpital Debrousse, Lyon; [8]Service de Génétique, Hôpital Nord, Saint-Etienne; [9]Service de Génétique, Hôpital Bretonneau, Tours

Hirschsprung disease (HSCR) is a common malformation of neural-crest–derived enteric neurons that is frequently associated with other congenital abnormalities. The *SMADIP1* gene recently has been recognized as disease causing in some patients with 2q22 chromosomal rearrangement, resulting in syndromic HSCR with mental retardation, with microcephaly, and with facial dysmorphism. We screened 19 patients with HSCR and mental retardation and eventually identified large-scale *SMADIP1* deletions or truncating mutations in 8 of 19 patients. These results allow further delineation of the spectrum of malformations ascribed to *SMADIP1* haploinsufficiency, which includes frequent features such as hypospadias and agenesis of the corpus callosum. Thus, *SMADIP1,* which encodes a transcriptional corepressor of Smad target genes, may play a role not only in the patterning of neural-crest–derived cells and of CNS but also in the development of midline structures in humans.

Hirschsprung disease (HSCR [MIM 142623]), the most common (1/5,000 live births) malformative cause of intestinal obstruction, has a complex inheritance and is frequently associated with other congenital abnormalities (Lyonnet et al. 2001). In particular, the combination of severe mental retardation, postnatal microcephaly, epilepsy, and facial dysmorphism has been recently recognized as an independent syndrome (Mowat et al. 1998). This syndrome has occasionally been ascribed to an interstitial deletion of chromosome 2q22 (Lurie et al. 1994; Mowat et al. 1998). Most recently, two de novo translocations—46,XX,t(2;13)(q22;q22) (Wakamatsu et al. 2001) and 46,XY,t(2;11)(q22.2;q21) (Cacheux et al. 2001)—allowed the identification of the gene encoding Smad-interacting protein 1 (SMADIP1 [MIM 605802]) as the disease-causing gene in this syndrome.

Yet, the prevalence of *SMADIP1* mutations and the spectrum of their clinical manifestations have remained ignored. Starting with a series of 250 nonfamilial cases of HSCR, we screened 19 unrelated patients with mental retardation, for possible *SMADIP1* mutations. Here, we report large-scale *SMADIP1* deletions or truncating mutations in ~50% (8 of 19) of these patients. Hypospadias and agenesis of the corpus callosum were frequently observed, allowing further delineation of this syndrome and suggesting that Smadip1 may play a role not only in the patterning of neural-crest–derived cells and of CNS but also in the development of midline structures in humans.

Nineteen patients from a larger series, of 250 patients with HSCR, were included in the series that we studied, on the basis of the following criteria: (1) normal chromosome analysis on standard examination, (2) moderate-to-severe mental retardation, and (3) either facial dysmorphism, cerebral anomaly including seizures, microcephaly, or agenesis of the corpus callosum. All

Received June 13, 2001; accepted for publication August 28, 2001; electronically published October 10, 2001.

Address for correspondence and reprints: Dr. S. Lyonnet, Département de Génétique, Hôpital Necker-Enfants Malades, 149, rue de Sèvres, 75743 Paris Cedex 15, France. E-mail: lyonnet@necker.fr

0002-9297/2001/6906-0021$02.00

patients were sporadic cases born of healthy, nonconsanguineous parents. Short-segment and long-segment HSCR were found in six and four patients, respectively, whereas the length of aganglionosis was not known in eight patients; finally, one patient (patient S.272) with severe constipation was included in the series, although HSCR was not confirmed. The detailed clinical findings regarding these 19 patients are summarized in table 1. Patient S.179 has been described elsewhere (Tanaka et al. 1993). Blood samples were obtained with informed consent, and DNA was extracted according to standard protocols.

Chromosomal analyses (RTBG [R-bands by Thymidine and BrdU by use of Giemsa], 400- and/or 850-bands resolution) were performed for all patients. FISH was performed using BAC RPCI-11 95O9 (GenBank accession AC010130), which contains most of *SMADIP1*. DNA of BAC RPCI-11 95O9 was labeled by nick translation by standard protocol, with incorporation of fluorescein isothiocyanate–dUTP (fig. 1). A control probe was prepared from PAC RPCI-1 164D18 (7qter; Knight et al. 2000), labeled with tetramethyl-rhodamine-dUTP. Hybridization on patients' metaphases was performed over 48 h. After a washing, chromosomes were counterstained using di-amidino-phenyl-indole. Metaphases were examined on a Leica DMRXA epifluorescent microscope. Images were captured and processed using the Leica QFISH software.

To detect infracytogenetic deletions of chromosome 2q22, five poly(CA) microsatellite markers flanking the *SMADIP1* locus were tested on the patients and their parents (fig. 2; primer sequences are available from the Genome Database). Moreover, real-time semiquantitative PCR at the *SMADIP1* locus was performed by hot-start PCR in glass capillaries by use of the LightCycler FastStart DNA Master SYBR Green I kit (Roche). The amplification was performed using primers encoding exon 6 of *SMADIP1* (table 2). Exon 3 of the *GDNF* gene on chromosome 5 was used as a control (forward, ATGTCACTGACTTGGGTCTG; and reverse, TGCACTGTAGCAGGAATGC). The PCR mixture contained 50 ng leukocyte DNA, 5 pmol each primer, and 2 μl reaction mixture, in a final volume of 20 μl (3 mM $MgCl_2$). Forty cycles of amplification were performed, each cycle consisting of 15 s denaturation at 95°C, 10 s annealing at 50°C, and 30 s elongation at 72°C. After amplification, a melting curve was performed (10 s at 95°C, 20 s at 65°C, and a slow dehybridization step at

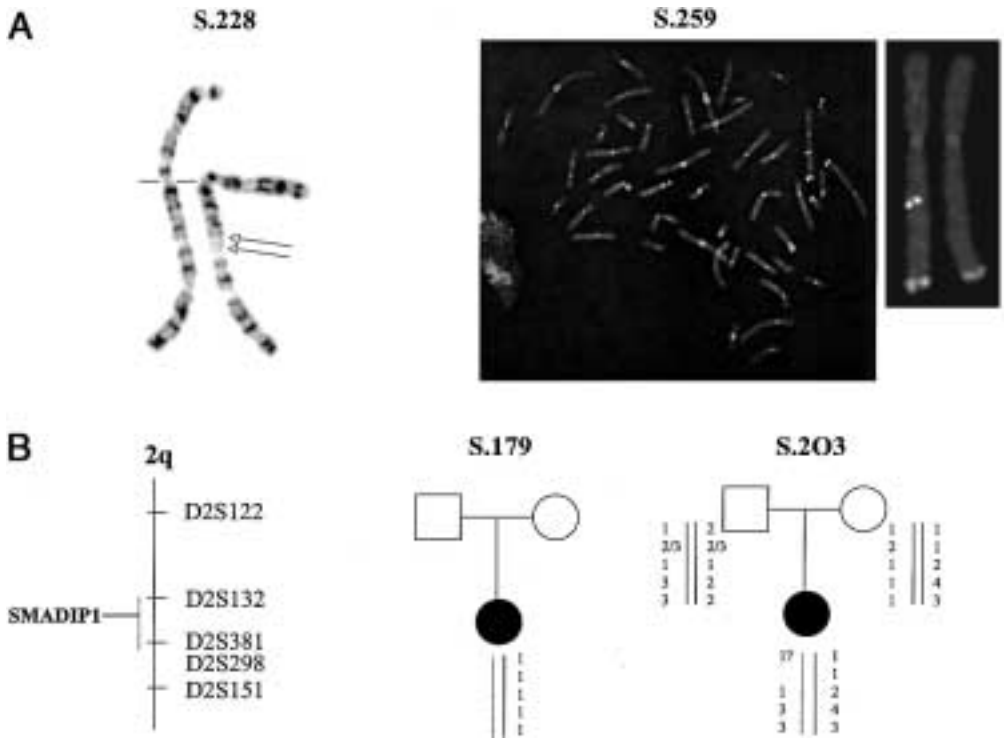

Figure 1 *SMADIP1* deletions. *A*, Chromosome 2 of patient S.228 and FISH analysis of patient S.259. *Left*, RTBG karyotype, showing chromosome 2 at 850-band resolution for patient S.228. *Right*, Metaphase of patient S.259, hybridized with probes BAC 95O9 (*SMADIP1*) and PAC 164D18 (7qter) as control. *B*, Haplotype analysis at *SMADIP1* locus in patients S.179 and S.203. The poly(CA) microsatellite markers used (and genetic distances [in cM]) are as follows: cen-D2S122-(1.2)-D2S132-(0.5)-D2S381-(0.6)-[D2S298-(?)]-D2S151-tel. *SMADIP1* lies between D2S132 and D2S381.

Table 1

Clinical Findings, at the *SMADIP1* Locus, in the Series of 19 Patients Studied

	Status of Patient[a]																		
Phenotype	S.99	S.103	S.107	S.166	S.167	S.177	S.179	S.184	S.203	S.226	S.228	S.230	S.233	S.238	S.259	S.264	S.266	S.272	S.273
Sex	M	M	M	M	M	M	F	F	F	?	M	F	F	M	F	M	F	F	M
HSCR[b]	+	+	SS	+	+	LS	+	LS	SS	+	SS	SS	SS	SS	LS	+	LS	−	+
Neurological findings:																			
Postnatal microcephaly	?	+	+	−	−	?	+	−	+	+	+	?	−	?	+	?	?	+	+
Agenesis of corpus callosum	+	+	+	−	−	?	−	−	+	?	+	−	−	−	+	−	?	+	−
Epilepsy	?	?	+	−	+	+	+	−	+	?	+	−	−	+	+	−	?	+	+
Mental retardation[c]	++	++	++	+	++	++	++	+	++	?	++	++	+	+	++	+	+	++	++
Facial dysmorphism:	?	+	+	−	−	+	+	−		?	+	+	?	−	+	−	−	+	+
Eye region[d]		+	+			+	+		?		+	+	+		+			+	+
Saddle nose		+	+			+	+		?		+	+	−		+			+	+
Ears[e]		+	+			+	+		?		+	+	−		+			+	+
Pointed chin		+	+			+	+		?		+	+	−		+			+	+
Heart defect	+	−	−	−	−	−	+	+	+	+	+	+	−	+	+	+	−	−	+
Hypospadias[f]	?	+	−	−	−	+	NR	NR	NR	−	+	NR	NR	−	NR	+	NR	NR	+
Renal anomalies	?	−	+	−	−	−	−	−	−	−	−	+	−	−	−	−	+	−	+
Pyloric stenosis	?	+	−	−	−	−	−	−	−	−	−	+	−	−	−	+	−	−	−
SMADIP1 mutation	−	+	+	−	−	−	+	−	+	−	+	+	−	−	+	−	−	+	−

[a] + = Affected; − = unaffected; ? = unknown.

[b] SS = short-segment HSCR; LS = long-segment HSCR.

[c] + = Mild-to-moderate mental retardation; ++ = severe mental retardation.

[d] Characterized by sunken eyes, downward-slanting palpebral fissures, strabismus, epicanthic fold, and thick eyebrows.

[e] Characterized by rotated ears with uplifted, fleshy earlobes and by thick antihelix.

[f] NR = not relevant.

65°C–95°C). Analysis was performed using the LightCycler software (second-derivate–maximum method).

The *SMADIP1* coding sequence and flanking introns were PCR amplified using a set of 15 primer pairs (exons 2–10; table 2) and were analyzed by silver-staining SSCP. When an abnormal SSCP pattern was identified, genomic DNA was sequenced on both strands by the fluorometric method (Big Dye Terminator Cycle Sequencing kit; Applied Biosystems) (fig. 3).

An interstitial deletion of chromosome 2q22 was observed on high-resolution karyotype in patient S.228 (fig. 1*A*). In addition, FISH analysis showed the presence of a deletion encompassing the *SMADIP1* locus in patient S.259 (fig. 1*A*). Finally, loss of heterozygosity at the *SMADIP1* locus suggested a submicroscopic deletion in two further patients (patients S.179 and S.203; fig. 1*B*). To demonstrate further evidence of a *SMADIP1* deletion in those patients, real-time semiquantitative PCR was performed. A significant retardation in the appearance of the amplification product (crossing point for exon 6 of *SMADIP1*) was observed in patients when compared with controls (table 3). This further strengthens the evidence of *SMADIP1* deletions in patients S.179 and S.203 (fig. 1*B* and table 3). *SMADIP1* deletions occurred de novo in three cases, and, in patients S.203 and S.259, results indicated that the deletion was carried by a paternal chromosome 2. In conclusion, in our series, 4 of 19 patients harbor a large-scale deletion encompassing the *SMADIP1* locus.

Nucleotide variations were identified in 4 of 19 patients (fig. 3 and table 4) and consistently involved the large exon 8 of *SMADIP1* (1,969 bp; 60% of the coding sequence). The mutations included a nonsense mutation (1685T→G [L562X]), 1-bp deletions or insertion (935delG, 1805delA, or 2453insT) that resulted in a frameshift, and a premature translation termination (at positions 337, 606, or 840 for the 935delG, 1805delA, or 2453insT mutations, respectively; fig. 4). Thus, in

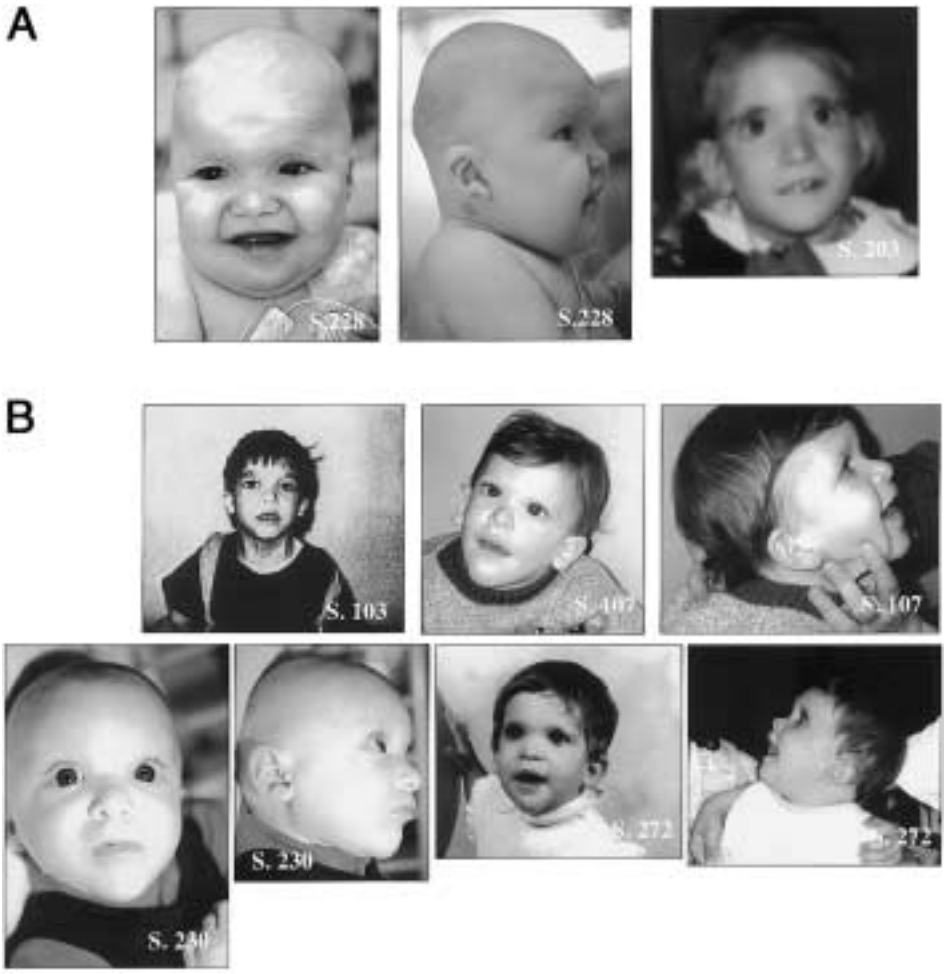

Figure 2 Frontal and profile views of patients presenting with either deletion (*A*) or mutation (*B*) of *SMADIP1*. In the frontal views, note long face with pointed chin, bushy eyebrows, sunken eyes, strabismus, epicanthic folds, saddle nose, thick helix, and fleshy, uplifted earlobes. In the profile views, note sunken eyes, saddle nose, thick helix, and fleshy, uplifted earlobes.

Table 2

Primers and PCR Conditions Used for the *SMADIP1*-Coding-Sequence Screening

Exon	Primer		Annealing Temperature (°C)	PCR Product (bp)
	Forward	Reverse		
2	GCGATGCCCACATTGTCG	TCTCGAGCCGCGTAGTG	53	229
3	ATCTCAACAGAGTGTTTAGAG	GAAGATGTGAAGATGGTAC	50	354
4	TGTGCTTGGCATGCTTAG	CATGACACAGGACAAATG	50	191
5	GAGATGGACTTGGGATCC	CAGAGGTCAGTGCAGTG	57[a]	297
6	GCTGCCATTGATTTACTG	GCCAATCAAAGCAATATCG	50	348
7	TTCCTCCTGCACAAAACTG	AAATGCAAATGCGAGCTCC	50	191
8:				
A	ATCAAGGAAATGTAACGG	GTGTGTAGCCATAAGAAC	50	346
B	CTGAACAGACAGGCTTAC	TGACTCACTACCGGAAG	50	411
C	GAGGAACAAGGAGTTAC	CTCAGAAAGTACAGATGAC	50	434
D	CCAACAAAGCCGGAGTT	TGTTAGCCTGAGAGGAG	56[b]	421
E	CATCACCATCTATAGCAG	CTGAACACTGGGTTAGTG	50	438
F	TGAGCCTCTGAACTTGAC	GCCACCTCTTTTCTTCATAG	53	361
9	GTGAGCACAAAGAGAAGC	GAAATGTACAGCAGGACG	50	284
10:				
A	CTAATCACCCTGTCATC	TAATGCTCTGCAAGTAAGC	53	317
B	GAAAGGGCACTTGGAAC	CAGCAGTGTTTTCAAGC	50	427

NOTE.—For PCR amplification, the reaction mixture (25 μl) contained 100 ng leukocyte DNA, 20 pmol each primer, 0.1 μM dNTP, 0.75 μl $MgCl_2$ 0.1 M, and 1 U *Taq* DNA polymerase (Gibco). Thirty cycles of amplification were performed, each cycle consisting of 30 s denaturation at 96°C, 30 s annealing, and 30 s elongation. PCR products were heated for 10 min at 96°C, loaded onto a GeneGel Excel 12.5/24 kit (Amersham Pharmacia Biotech), and electrophoresed for 2.5 h at 5°C and at 15°C.

[a] + 5% Dimethyl sulfoxide.

[b] + 2.5% Dimethyl sulfoxide.

all patients, the three carboxy-terminal zinc-finger domains (C-ZFD; fig. 4) of SMADIP1 were presumably deleted in the mutant gene products. In addition, the 935delG mutation disrupted the fourth amino-terminal zinc-finger domain (N-ZFD; fig. 4) and the Smad-binding domain (SBD; fig. 4) of the protein. In three of four patients, the *SMADIP1* mutation was found to have occurred de novo (parents of patient S.103 were not available for study; data not shown).

Dysmorphic facial features were studied in the eight patients carrying *SMADIP1* deletions or mutations. Consistent features included sunken eyes, down-slant-

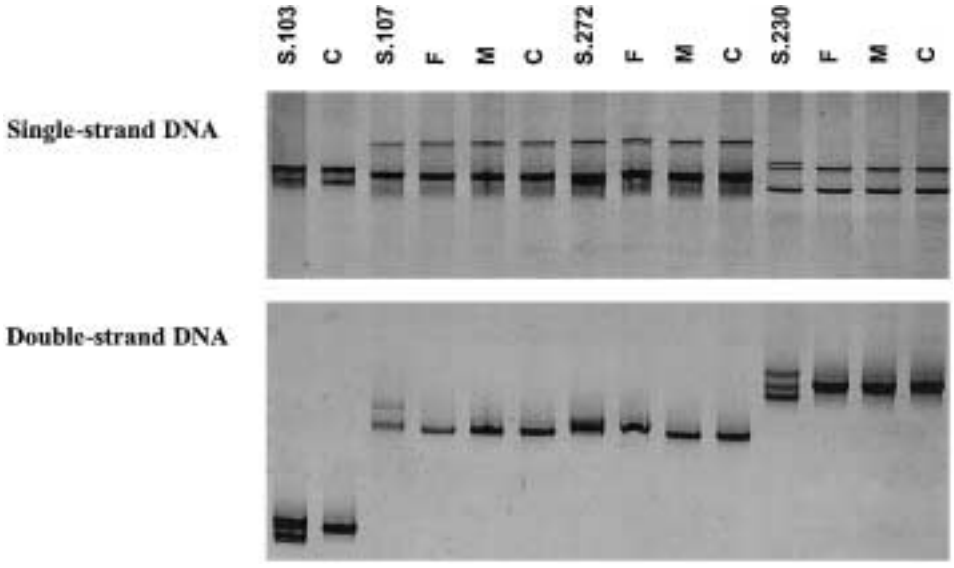

Figure 3 SSCP patterns in patients S.103, S.107, S.230, and S.272. Note the abnormal SSCP pattern in the patients, as compared to their fathers (F) and mothers (M) and to controls (C).

Table 3

Results of Real-Time Semiquantitative PCR of *SMADIP1*, with *GDNF* as a Control

Source	Crossing Point (SD)		Δ1[a]	Δ2[b]
	SMADIP1	*GDNF*		
Patient S.179	23.95 (.044)	21.65 (.068)	2.3	1.23
Patient S.203	22.89 (.046)	19.92 (.1)	2.97	1.9
Father of patient S.203	21.56 (.081)	20.81 (.038)	.75	.3
Mother of patient S.203	21.21 (.098)	20.66 (.093)	.55	.5
Patient S.228	22.85 (.062)	20.65 (.014)	2.2	1.13
Patient S.259	22.59 (.075)	20.19 (.026)	2.4	1.33
Mother of patient S.259	22.04 (.089)	20.63 (.028)	1.4	.33
Controls (n = 2)	22.41 (.075)	21.34 (.075)	1.07	…

[a] Δ1 = Difference, in crossing point, between *SMADIP1* and the control gene, *GDNF*.

[b] Δ2 = Difference, in Δ1, between tested individuals and controls.

ing palpebral fissures, strabismus, thick eyebrows with lateral flaring, saddle nose, pointed chin, thick antihelix, and rotated ears with uplifted, fleshy earlobes (fig. 2); the patients' hands were slender, with tapered fingers. Interestingly, a significant proportion of patients presented with an agenesis of the corpus callosum (six of eight), urogenital anomalies (four of eight), or cardiac defects (five of eight), but no correlation between the mutant phenotype and the clinical symptoms could be found in our series (table 4). In particular, no clear phenotypic differences were observed between patients with a large-scale deletion and patients with intragenic truncating mutations. Conversely, most *SMADIP1*-mutation–negative patients did not share significant phenotypic features.

Here, we report large-scale deletions or mutations of *SMADIP1* in eight patients presenting with a syndromic form of HSCR characterized by severe mental retardation, by dysmorphic facial features, and by midline defects. *SMADIP1* has been isolated in mouse embryo by the yeast two-hybrid system in the search for Smad-interacting proteins (Verschueren et al. 1999). Smadip1 is a member of the δ-EF1/Zfh-1 family and harbors a homeodomain-like sequence and a Smad-binding domain flanked by two clusters of zinc-finger sequences that are both required for transcriptional repression of receptor-activated Smad target genes (Remacle et al. 1999; fig. 4).

Mowat et al. (1998) were the first to point out the clinical heterogeneity among patients with syndromic HSCR with postnatal microcephaly and mental retardation (Mowat et al. 1998). They eventually identified a subgroup of patients who shared characteristic dysmorphic facial features, seizures, failure to thrive, and congenital cardiac defect (Mowat et al. 1998). In one case, chromosomal analysis revealed an interstitial deletion of chromosome 2q21-q23. Most recently, *SMADIP1* was identified as the disease-causing gene in this syndrome (Cacheux et al. 2001; Wakamatsu et al. 2001).

All mutant genotypes in our series were heterozygous and were expected to produce a truncated or absent Smadip1 protein. These data suggest that loss of function (haploinsufficiency) at the *SMADIP1* locus is the most likely disease-causing mechanism. Moreover, since patients with *SMADIP1* mutations have the same clinical features as are observed in patients with large-scale deletions, the involvement of a contiguous gene(s) is unlikely. Finally, all mutations reported here occurred de novo, an observation that is in agreement with a very severe phenotype in heterozygotes.

Comparison of the patients whom we studied with those previously reported to harbor a *SMADIP1* mutation allows further delineation of the clinical profile of this novel syndromic HSCR entity. In particular, as frequent

Table 4

Patients Presenting with a *SMADIP1* Anomaly

Patient (Sex)	Agenesis of Corpus Callosum?	Cardiac Defect[a]	Genital Anomaly[b]	Renal Anomaly[c]	*SMADIP1* Deletion (Method[s])[d]	*SMADIP1* Mutation
S.103 (M)	Yes	…	Hypospadias	?	…	935delG
S.107 (M)	Yes	…	Cryptorchidism	VUR	…	1805delA
S.179 (F)	No	PDA, ASD	NR	…	Deletion (MA, RS-PCR)	…
S.203 (F)	Yes	ASD	NR	?	Deletion (MA, RS-PCR)	…
S.228 (M)	Yes	VSD	Hypospadias, cryptorchidism	?	Deletion (CS, RS-PCR)	…
S.230 (F)	No	ASD, VSD, PS	NR	Hydronephrosis	…	2453insT
S.259 (F)	Yes	AC	NR	?	Deletion (MA, FISH, RS-PCR)	…
S.272 (F)	Yes	…	NR	…	…	1685T→G (L562X)

[a] PDA = patent ductus arteriosus; ASD = atrial septal defect; VSD = ventricular septal defect; PS = pulmonary stenosis; AC = aortic coarctation.

[b] NR = not relevant.

[c] VUR = vesico ureteral reflux.

[d] MA = microsatellite analysis; RS-PCR = real-time semiquantitative PCR; CS = cytogenetic studies.

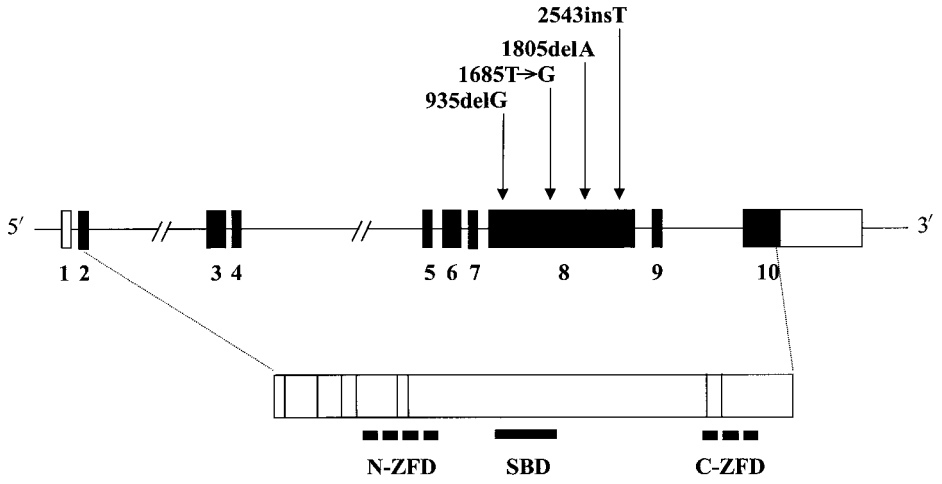

Figure 4 *SMADIP1* gene structure. *Top*, Genomic structure. The *SMADIP1* mutations identified are shown by downward-pointing arrows. *Bottom*, SMADIP1 protein. The four N-terminal and three C-terminal zinc-finger domains (N-ZFD and C-ZFD, respectively), as well as the Smad-binding domain (SBD), are indicated.

features in this syndrome, it is possible to include congenital defects of cardiac septation (in 62% of patients), agenesis of the corpus callosum (in 50% of patients), and hypospadias (table 4) (Lurie et al. 1994; Mowat et al. 1998; Wakamatsu et al. 2001). It is notable that all three features result from defects in midline development. Renal abnormalities (in three patients) and pyloric stenosis (in two patients) are also notable. Conversely, the MCA-MR (multiple-congenital-abnormalities–mental-retardation) syndrome, referred to as "Goldberg-Shprintzen syndrome" (MIM 235730), with HSCR, mental retardation, and cleft palate is clearly a different condition, both on the basis of clinical criteria and on the basis of mode of inheritance (autosomal recessive). In the literature, three patients reported to have had Goldberg-Shprintzen syndrome most likely presented with the syndromic HSCR accounted for by *SMADIP1* mutations (Hurst et al. 1988, case 3; Tanaka et al. 1993, patient S.179; Ohnuma et al. 1997). It would be interesting to either confirm or exclude this hypothesis by studying *SMADIP1* in families with Goldberg-Shprintzen syndrome.

Whole-mount in situ hybridization in *Xenopus* showed an early *SMADIP1* expression in the dorsal ectoderm and, later, in the dorsal neural tube and neural crests. In addition, over-expression of *SMADIP1* has led to an enlargement of neural tissues and to ocular malformations (Eisaki et al. 2000). Thus, *SMADIP1* could be regarded as pleiotropic. Our data support these findings and suggest that Smadip1 is involved not only in neural-crest–derived cells (in the enteric nervous system and craniofacial mesectoderm) and in the CNS but also in heart septation (patent ductus arteriosus, as well as ventricular and atrial septal defects) and development of midline structures (corpus callosum and genitalia). Therefore, although the putative involvement of *SMADIP1* in renal anomalies and in pyloric stenosis needs further documentation, the expression pattern in human embryo and the identification of SMADIP1 target genes should be regarded as important.

Finally, the syndromic HSCR entity discussed in this study (which, for clarity, we suggest should be named after Lurie and Mowat) may be regarded as a recognizable entity even in the absence of biopsy-proved HSCR, as in one of the patients whom we studied (S.272). Thus, this syndrome may be found to occur with greater frequency than was originally expected, and we believe that *SMADIP1* mutations should be searched for in patients with mental retardation, microcephaly, and agenesis of the corpus callosum only. This hypothesis is currently under investigation.

Acknowledgments

We would like to thank I. Allart (Resource Center/Primary Database of the German Human Genome Project), for providing the RPCI-11 95O9 BAC with celerity, and C. Ozilou and M. Le Lorc'h, for their help in FISH experiments. This work was supported by Fondation pour la Recherche Médicale grant ARS 2.13, by a grant from INSERM and Association Française contre les Myopathies (Réseau de Recherche sur les Maladies Rares 2000), and by European Community grant QLRT-2000-01648.

Electronic-Database Information

Accession numbers and URLs for data in this article are as follows:

GenBank, http://www.ncbi.nlm.nih.gov/Genbank/ (for BAC RPCI-11 95O9 [accession number AC010130])

Genome Database, The, http://gdbwww.gdb.org/ (for primer sequences)

Online Mendelian Inheritance in Man (OMIM), http://www.ncbi.nlm.nih.gov/Omim/ (for HSCR [MIM 142623], SMADIP1 [MIM 605802], and Goldberg-Shprintzen syndrome [MIM 235730])

References

Cacheux V, Dastot-Le Moal F, Kääriäinen H, Bondurand N, Rintala R, Boissier B, Wilson M, Mowat D, Goossens M (2001) Loss-of-function mutations in *SIP1* Smad interacting protein 1 result in a syndromic Hirschsprung disease. Hum Mol Genet 14:1503–1510

Eisaki A, Kuroda H, Fukui A, Asashima M (2000) *XSIP1*, a member of two-handed zinc finger proteins, induced anterior neural markers in *Xenopus laevis* animal cap. Biochem Biophys Res Commun 271:151–157

Hurst JA, Markiewicz M, Kumar D, Brett EM (1988) Unknown syndrome: Hirschsprung's disease, microcephaly, and iris coloboma: a new syndrome of defective neuronal migration. J Med Genet 25:494–497

Knight SJ, Lese CM, Precht KS, Kuc J, Ning Y, Lucas S, Regan R, Brenan M, Nicod A, Lawrie NM, Cardy DL, Nguyen H, Hudson TJ, Riethman HC, Ledbetter DH, Flint J (2000) An optimized set of human telomere clones for studying telomere integrity and architecture. Am J Hum Genet 67:320–332

Lurie IW, Supovitz KR, Rosenblum-Vos LS, Wulfsberg EA (1994) Phenotypic variability of del(2) (q22-q23): report of a case with a review of the literature. Genet Couns 5:11–14

Lyonnet S, Chakravarti A (2001) Hirschsprung disease. In: Scriver CR, Beaudet AL, Sly WS, Valle D (eds) The metabolic and molecular bases of inherited diseases, 8th ed. McGraw-Hill, New York, pp 6231–6255

Mowat DR, Croaker GD, Cass DT, Kerr BA, Chaitow J, Ades LC, Chia NL, Wilson MJ (1998) Hirschsprung disease, microcephaly, mental retardation, and characteristic facial features: delineation of a new syndrome and identification of a locus at chromosome 2q22-q23. J Med Genet 35:617–623

Ohnuma K, Imaizumi K, Masuno M, Nakamura M, Kuroki Y (1997) Magnetic resonance imaging abnormalities of the brain in Goldberg-Shprintzen syndrome (Hirschsprung disease, microcephaly, and iris coloboma). Am J Med Genet 73:230–232

Remacle JE, Kraft H, Lerchner W, Wuytens G, Collart C, Verschueren K, Smith JC, Huylebroeck D (1999) New mode of DNA binding of multi-zinc finger transcription factors: δEF1 family members bind with two hands to two target sites. EMBO J 18:5073–5084

Tanaka H, Ito J, Cho K, Mikawa M (1993) Hirschsprung disease, unusual face, mental retardation, epilepsy, and congenital heart disease: Goldberg-Shprintzen syndrome. Pediatr Neurol 9:479–481

Verschueren K, Remacle JE, Collart C, Kraft H, Baker BS, Tylzanowski P, Nelles L, Wuytens G, Su MT, Bodmer R, Smith JC, Huylebroeck D (1999) SIP1, a novel zinc finger/homeodomain repressor, interacts with Smad proteins and binds to 5′-CACCT sequences in candidate target genes. J Biol Chem 274:20489–20498

Wakamatsu N, Yamada Y, Yamada K, Ono T, Nomura N, Taniguchi H, Kitoh H, Mutoh N, Yamanaka T, Mushiake K, Kato K, Sonta S, Nagaya M (2001) Mutations in *SIP1*, encoding Smad interacting protein-1, cause a form of Hirschsprung disease. Nat Genet 27:369–370